

Feasibility and physics potential of detecting ^8B solar neutrinos at JUNO

Jie Zhao^{a,*} **on behalf of the JUNO Collaboration**

(a complete list of authors can be found at the end of the proceedings)

^a*Institute of High Energy Physics, Beijing, China*

E-mail: zhaojie@ihep.ac.cn

The Jiangmen Underground Neutrino Observatory (JUNO) features a 20 kt multi-purpose underground liquid scintillator sphere as its main detector. In this talk we describe in detail a comprehensive assessment of JUNO's potential for detecting ^8B solar neutrinos via the neutrino-electron elastic scattering process. A reduced 2 MeV threshold for the recoil electron energy is achievable with optimized background reduction strategies. With ten years of data taking, about 60,000 signal and 30,000 background events are expected. This leads to a simultaneous measurement of $\sin^2 \theta_{12}$ and Δm_{21}^2 using reactor antineutrinos and solar neutrinos in the JUNO detector. This large sample will enable an examination of the distortion of the recoil electron spectrum that is dominated by the neutrino flavor transformation in the dense solar matter. If $\Delta m_{21}^2 = 4.8 \times 10^{-5} (7.5 \times 10^{-5} \text{ eV}^2)$, JUNO can provide evidence of neutrino oscillation in the Earth at approximately the 3σ (2σ) level by measuring the non-zero signal rate variation with respect to the solar zenith angle. Moreover, JUNO can simultaneously measure Δm_{21}^2 using ^8B solar neutrinos to a precision of 20% or better, depending on the central value, and to sub-percent precision using reactor antineutrinos. A comparison of these two measurements from the same detector will help understand the current mild inconsistency between the value of reported by solar neutrino experiments and the KamLAND experiment.

*37th International Cosmic Ray Conference (ICRC 2021)
July 12th – 23rd, 2021
Online – Berlin, Germany*

*Presenter

1. Introduction

Solar neutrinos, produced during nuclear fusion in the solar core, have played an important role in the history of neutrino physics. The standard scenario of three neutrino mixing predicts a smooth upturn in the survival probability (P_{ee}) in the neutrino energy region between the high (MSW dominated) and low (vacuum dominated) ranges, and a sizable Day-Night asymmetry at the percentage level. The combined Super-K and SNO fitting favors $\Delta m_{21}^2 = 4.8 \times 10^{-5} \text{ eV}^2$ [1], while KamLAND gives $\Delta m_{21}^2 = 7.53 \times 10^{-5} \text{ eV}^2$ [2]. From the latest results at the Neutrino 2020 conference [3], the inconsistency is reduced from 2σ to around 1.4σ due to the larger statistics and the update of analysis methods.

Determining whether this inconsistency is a statistical fluctuation or a physical effect beyond the standard neutrino oscillation framework requires further measurements. The Jiangmen Underground Neutrino Observatory (JUNO), a 20 kt multi-purpose underground liquid scintillator (LS) detector, can simultaneously measure Δm_{21}^2 using ${}^8\text{B}$ solar neutrinos reactor antineutrinos. The analysis threshold for the recoil electrons can be decreased to 2 MeV, assuming an achievable intrinsic radioactivity background level and better muon veto strategies. The lower threshold leads to larger signal statistics and a more sensitive examination of the spectrum distortion of recoil electrons. New measurement of the non-zero signal rate variation versus the solar zenith angle (Day-Night asymmetry) is also expected. After combining with the ${}^8\text{B}$ neutrino flux from the SNO NC measurement, the Δm_{21}^2 precision is expected to be similar to the current global fitting results [4].

2. Solar neutrino detection at JUNO

In LS detectors, the primary detection channel for solar neutrinos is their elastic scattering with electrons. In this study, we assume an arrival ${}^8\text{B}$ neutrino flux of $(5.25 \pm 0.20) \times 10^6 / \text{cm}^2 / \text{s}$ provided by the NC channel measurement at SNO [5]. The ${}^8\text{B}$ neutrino spectra and shape uncertainties are taken from Refs. [6, 7] as shown in the left figure 1. Taking the MSW effects in both the Sun and the Earth into consideration, the ν_e survival probabilities (P_{ee}) with respect to the neutrino energy for the two Δm_{21}^2 values are shown in the right figure 1.

After scattering, the total energy and momentum of the neutrino and electron are redistributed. The expected signal rate in the full energy range is 4.15 (4.36) counts per day per kt (cpd/kt) for $\Delta m_{21}^2 = 4.8(7.5) \times 10^{-5} \text{ eV}^2$.

3. Background budget

3.1 Internal radioactivity

As a feasibility study, we start with 10^{-17} g/g U and Th in the secular equilibrium, which are close to those of Borexino Phase I [8]. The top plot of figure 2 shows the internal background spectrum under the assumptions above. The background can be further reduced by the time, space, and energy correlation from the Bi-Po/Bi-Tl cascade decays, and the results are shown in the bottom plot of figure 2.

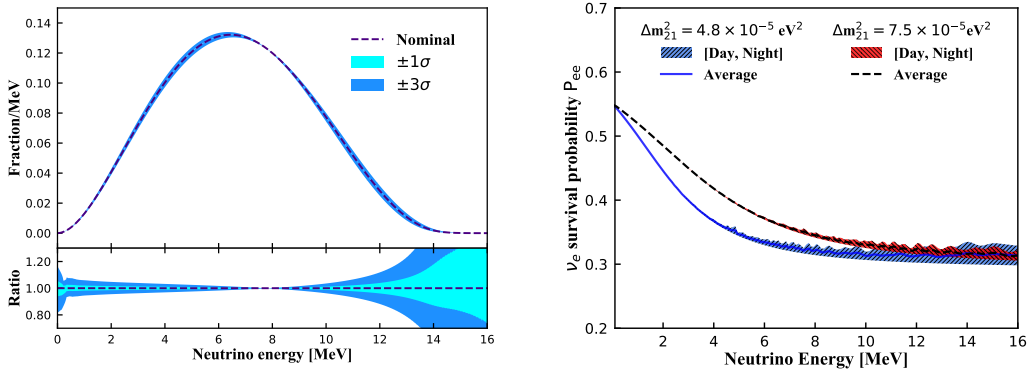


Figure 1: Left: ${}^8\text{B}$ ν_e spectrum together with the shape uncertainties. The data are taken from Ref.[26]. Right: Solar ν_e survival probabilities (P_{ee}) with respect to the neutrino energy. The shadowed area shows the variation of at different solar zenith angles.

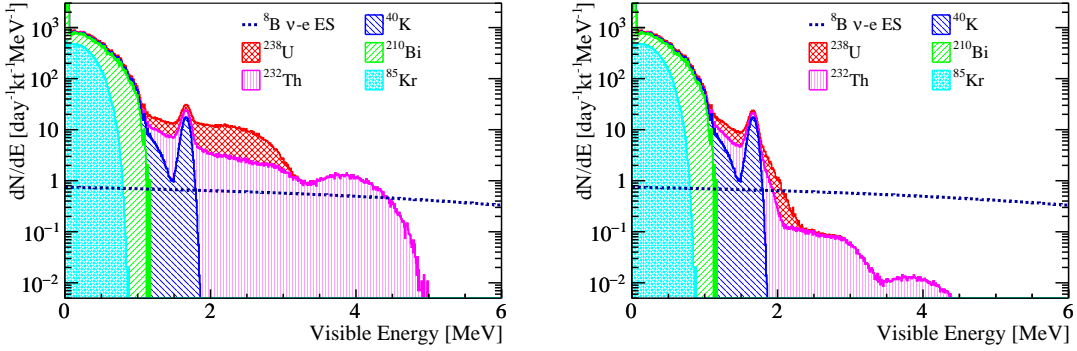


Figure 2: Internal radioactivity background compared with ${}^8\text{B}$ signal before (left) and after (right) time, space, and energy correlation cuts to remove the Bi-Po/Bi-Tl cascade decays.

3.2 External radioactivity

All detector materials at JUNO have been carefully selected to fulfill radiopurity requirements. With the measured radioactivity values, a simulation is performed to obtain the external deposited energy spectrum in the LS. According to the simulation results, an energy dependent fiducial volume (FV) cut, in terms of the reconstructed radial position (r) in the spherical coordinate system, is designed as follows:

- $2 < E_{\text{vis}} \leq 3 \text{ MeV}, r < 13 \text{ m}, 7.9 \text{ kt target mass};$
- $3 < E_{\text{vis}} \leq 5 \text{ MeV}, r < 15 \text{ m}, 12.2 \text{ kt target mass};$
- $E_{\text{vis}} > 5 \text{ MeV}, r < 16.5 \text{ m}, 16.2 \text{ kt target mass}.$

In this way, the external radioactivity background is suppressed to less than 0.5% compared with the signals in the entire energy range, while the signal statistics are maximized at high energies.

3.3 Cosmogenic isotopes

The relatively shallow vertical rock overburden, approximately 680 m, leads to a 0.0037 Hz/m muon flux, with an averaged energy of 209 GeV. The direct consequence is approximately 3.6 Hz muons passing through the LS target. More than 10,000 ${}^{11}C$ isotopes are generated per day, which constrains the analysis threshold to 2 MeV, as shown in figure 3. Based on the simulation and measurements of previous experiments, it is found that other isotopes can be suppressed to a 1% level with a cylindrical veto along the muon track and the Three-Fold Coincidence cut (TFC) among the muon, the spallation neutron capture, and the isotope decay.

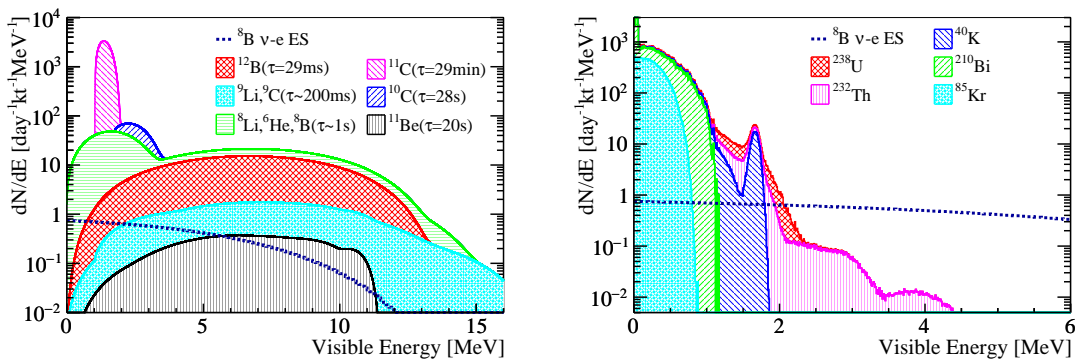


Figure 3: Cosmogenic background before (left) and after veto (right). The isotope yields shown here are scaled from the KamLAND’s [48] and Borexino’s measurements [49]. The huge amount of ${}^{11}C$ constrains the analysis threshold to 2 MeV. The others isotopes can be well suppressed with veto strategies discussed in the text.

4. Expected results

After applying all the selection cuts, about 60,000 recoil electrons and 30,000 background events are expected in 10 years of data taking as shown in figure 4.

4.1 Spectrum distortion test

A background-subtracted Asimov data set is produced in the standard LMA-MSW framework using different Δm_{21}^2 values, shown as the black dots and red line in the left figure 5. We would like to test an energy-independent hypothesis, where the P_{ee} is assumed as a flat value for neutrino energies larger than 2 MeV. This hypothesis is rejected at 2.7σ with $\Delta m_{21}^2 = 7.5 \times 10^{-5} \text{ eV}^2$.

4.2 Day-Night asymmetry

Solar neutrino propagation through the Earth is expected, via the MSW effect, to cause signal rate variation versus the solar zenith angle. This rate variation observable also provides additional sensitivity to the Δm_{21}^2 value, as shown in the right figure 5. The variation is quantified by defining the Day-Night asymmetry as:

$$A_{DN} = \frac{R_D - R_N}{(R_D + R_N)/2}, \quad (1)$$

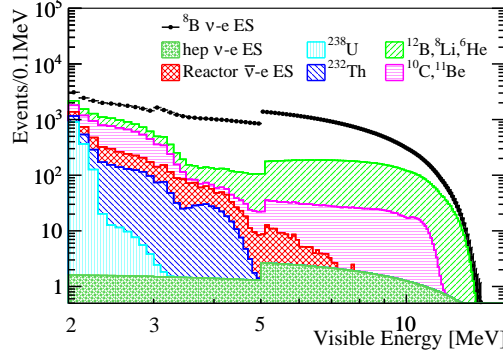


Figure 4: Expected signal and background spectra in ten years of data taking, with all selection cuts and muon veto methods applied.

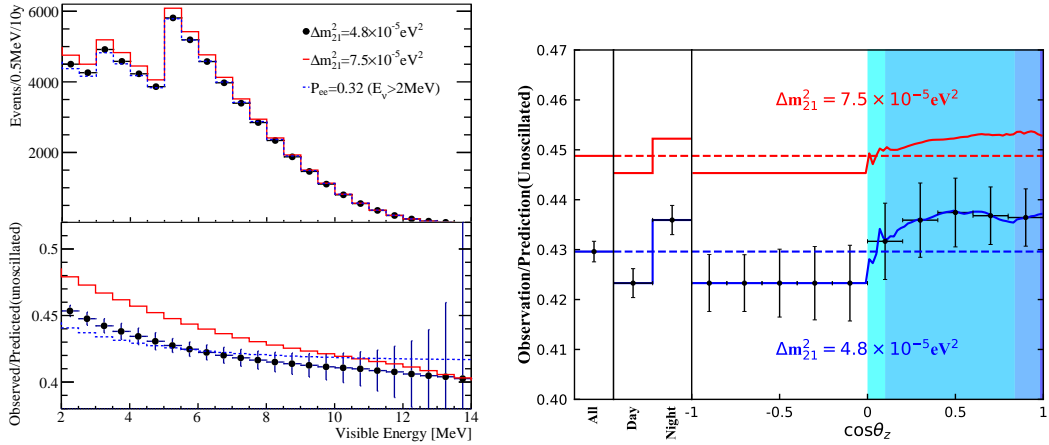


Figure 5: Left: Background subtracted spectra produced in the standard LMA-MSW framework for two Δm_{21}^2 values (black dots and red line, respectively), and the $P_{ee} = 0.32$ ($E_\nu > 2$ MeV) assumption (blue line). Their comparison with the no flavor conversion is shown in the bottom panel. Right: Ratio of ${}^8\text{B}$ neutrino signals produced in the standard LMA-MSW framework to the no-oscillation prediction at different solar zenith angles.

where R_D and R_N are the background-subtracted signal rates during the Day ($\cos \theta_z < 0$) and Night ($\cos \theta_z > 0$), respectively. Compared with Super-Kamiokande's results from Ref. [1], JUNO could reach the same precision of A_{DN} in less than 10 years.

4.3 Measurement of oscillation parameters

As mentioned above, in the standard neutrino oscillation framework, Δm_{21}^2 can be measured using the information in the spectra distortion and the signal rate variation versus solar zenith angle. With ten years of data taking the expected sensitivity of $\sin^2 \theta_{12}$ and Δm_{21}^2 is shown in Fig. 6.

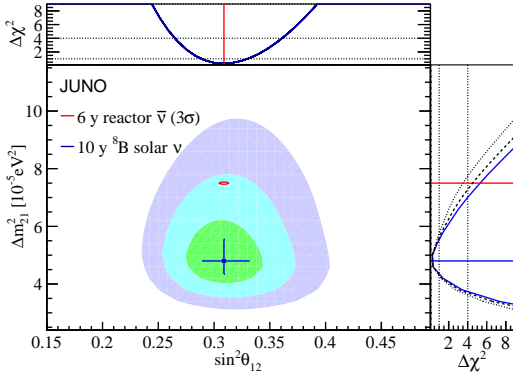


Figure 6: 68.3%, 95.5%, and 99.7% C.L. allowed regions in the $\sin^2 \theta_{12}$ and Δm_{21}^2 plane using the ${}^8\text{B}$ solar neutrino in ten years data taking. The one-dimensional $\Delta \chi^2$ for $\sin^2 \theta_{12}$ and Δm_{21}^2 are shown in the top and right panels, respectively.

5. Summary

The JUNO experiment, with a 20 kt LS detector, can shed light on the current inconsistency between Δm_{21}^2 values measured using solar neutrinos and reactor antineutrinos. A set of energy-dependent FV cuts is newly designed based on comprehensive background studies, leading to the maximized target mass with negligible external background. A set of distance-dependent veto time cuts are developed for the cylindrical veto along the muon track, resulting in a significantly improved signal to background ratio. In the standard three-flavor neutrino oscillation framework, the spectrum distortion and the Day-Night asymmetry lead to a Δm_{21}^2 measurement of $4.8^{+0.8}_{-0.5} (7.5^{+1.6}_{-1.2}) \times 10^{-5} \text{ eV}^2$, with a similar precision to the current solar global fitting result. Details of this study can be found in [9].

References

- [1] K. Abe *et al.*, Phys. Rev. D 94(5), 052010 (2016)
- [2] A. Gando *et al.*, Phys. Rev. D 88(3), 033001 (2013)
- [3] Yasuhiro Nakajima, Recent results and future prospects from Super-Kamiokande, Presentation at the XXIX International Conference on Neutrino Physics and Astrophysics (Neutrino 2020), June 2020
- [4] Ivan Esteban and M. C. Gonzalez-Garcia, JHEP 01, 106 (2019)
- [5] B. Aharmim *et al.*, Phys. Rev. C 88, 025501 (2013)
- [6] John N. Bahcall, E. Lisi, D. E. Alburger *et al.*, Phys. Rev. C 54, 411-422 (1996)
- [7] John N. Bahcall, Phys. Rev. C 56, 3391-3409 (1997)
- [8] C. Arpesella *et al.*, Phys. Rev. Lett. 101, 091302 (2008)
- [9] Angel Abusleme *et al.*, Chinese Phys. C 45 023004 (2021)

Full Authors List: JUNO Collaboration

Angel Abusleme⁵, Thomas Adam⁴⁵, Shakeel Ahmad⁶⁶, Rizwan Ahmed⁶⁶, Sebastiano Aiello⁵⁵, Muhammad Akram⁶⁶, Fengpeng An²⁹, Qi An²², Giuseppe Andronico⁵⁵, Nikolay Anfimov⁶⁷, Vito Antonelli⁵⁷, Tatiana Antoshkina⁶⁷, Burin Asavapibhop⁷¹, João Pedro Athayde Marcondes de André⁴⁵, Didier Auguste⁴³, Andrej Babic⁷⁰, Nikita Balashov⁶⁷, Wander Baldini⁵⁶, Andrea Barresi⁵⁸, Davide Basilico⁵⁷, Eric Baussan⁴⁵, Marco Bellato⁶⁰, Antonio Bergnoli⁶⁰, Thilo Birkenfeld⁴⁸, Sylvie Blin⁴³, David Blum⁵⁴, Simon Blyth⁴⁰, Anastasia Bolshakova⁶⁷, Mathieu Bongrand⁴⁷, Clément Bordereau^{44,40}, Dominique Breton⁴³, Augusto Brigatti⁵⁷, Riccardo Brugnera⁶¹, Riccardo Bruno⁵⁵, Antonio Budano⁶⁴, Mario Buscemi⁵⁵, Jose Bustos⁴⁶, Ilya Butorov⁶⁷, Anatael Cabrera⁴³, Hao Cai³⁴, Xiao Cai¹⁰, Yanke Cai¹⁰, Zhiyan Cai¹⁰, Riccardo Callegari⁶¹, Antonio Cammi⁵⁹, Agustin Campeny⁵, Chuanya Cao¹⁰, Guofu Cao¹⁰, Jun Cao¹⁰, Rossella Caruso⁵⁵, Cédric Cerna⁴⁴, Jinfan Chang¹⁰, Yun Chang³⁹, Pingping Chen¹⁸, Po-An Chen⁴⁰, Shaomin Chen¹³, Xurong Chen²⁶, Yi-Wen Chen³⁸, Yixue Chen¹¹, Yu Chen²⁰, Zhang Chen¹⁰, Jie Cheng¹⁰, Yaping Cheng⁷, Alexey Chetverikov⁶⁷, Davide Chiesa⁵⁸, Pietro Chimenti³, Artem Chukanov⁶⁷, Gérard Claverie⁴⁴, Catia Clementi⁶², Barbara Clerbaux², Selma Conforti Di Lorenzo⁴⁴, Daniele Corti⁶⁰, Flavio Dal Corso⁶⁰, Olivia Dalager⁷⁴, Christophe De La Taille⁴⁴, Jiawei Deng³⁴, Zhi Deng¹³, Ziyuan Deng¹⁰, Wilfried Depnerring⁵², Marco Diaz⁵, Xuefeng Ding⁵⁷, Yayun Ding¹⁰, Bayu Dirgantara⁷³, Sergey Dmitrievsky⁶⁷, Tadeas Dohnal⁴¹, Dmitry Dolzhikov⁶⁷, Georgy Donchenko⁶⁹, Jianmeng Dong¹³, Evgeny Doroshkevich⁶⁸, Marcos Dracos⁴⁵, Frédéric Druillole⁴⁴, Ran Du¹⁰, Shuxian Du³⁷, Stefano Dusini⁶⁰, Martin Dvorak⁴¹, Timo Enqvist⁴², Heike Enzmann⁵², Andrea Fabbri⁶⁴, Lukas Fajt⁷⁰, Donghua Fan²⁴, Lei Fan¹⁰, Jian Fang¹⁰, Wenxing Fang¹⁰, Marco Fargetta⁵⁵, Dmitry Fedoseev⁶⁷, Vladko Fekete⁷⁰, Li-Cheng Feng³⁸, Qichun Feng²¹, Richard Ford⁵⁷, Amélie Fournier⁴⁴, Haonan Gan³², Feng Gao⁴⁸, Alberto Garfagnini⁶¹, Arsenii Gavrikov⁶¹, Marco Giammarchi⁵⁷, Agnese Giaz⁶¹, Nunzio Giudice⁵⁵, Maxim Gonchar⁶⁷, Guanghua Gong¹³, Hui Gong¹³, Yuri Gornushkin⁶⁷, Alexandre Göttel^{50,48}, Marco Grassi⁶¹, Christian Grewing⁵¹, Vasily Gromov⁶⁷, Minghao Gu¹⁰, Xiaofei Gu³⁷, Yu Gu¹⁹, Mengyun Guan¹⁰, Nunzio Guardone⁵⁵, Maria Gui⁶⁶, Cong Guo¹⁰, Jingyuan Guo²⁰, Wanlei Guo¹⁰, Xinheng Guo⁸, Yuhang Guo^{35,50}, Paul Hackspacher⁵², Caren Hagner⁴⁹, Ran Han⁷, Yang Han²⁰, Muhammad Sohaib Hassan⁶⁶, Miao He¹⁰, Wei He¹⁰, Tobias Heinz⁵⁴, Patrick Hellmuth⁴⁴, Yuekun Heng¹⁰, Rafael Herrera⁵, YuenKeung Hor²⁰, Shaojing Hou¹⁰, Yee Hsiung⁴⁰, Bei-Zhen Hu⁴⁰, Hang Hu²⁰, Jianrun Hu¹⁰, Jun Hu¹⁰, Shouyang Hu⁹, Tao Hu¹⁰, Zhuojun Hu²⁰, Chunhao Huang²⁰, Guihong Huang¹⁰, Hanxiong Huang⁹, Wenhao Huang²⁵, Xin Huang¹⁰, Xingtiao Huang²⁵, Yongbo Huang²⁸, Jiaqi Hui³⁰, Lei Huo²¹, Wenju Huo²², Cédric Huss⁴⁴, Safeer Hussain⁶⁶, Ara Ioannissian¹, Roberto Isocrate⁶⁰, Beatrice Jelmini⁶¹, Kuo-Lun Jen³⁸, Ignacio Jeria⁵, Xiaolu Ji¹⁰, Xingzhao Ji²⁰, Huihui Jia³³, Junji Jia³⁴, Siyu Jian⁹, Di Jiang²², Wei Jiang¹⁰, Xiaoshan Jiang¹⁰, Ruyi Jin¹⁰, Xiaoping Jing¹⁰, Cécile Jollet⁴⁴, Jari Joutsenvaara⁴², Sirichok Junghawan⁷³, Leonidas Kalousis⁴⁵, Philipp Kampmann⁵⁰, Li Kang¹⁸, Rebin Karaparambil⁴⁷, Narine Kazarian¹, Khanchai Khosonthongkee⁷³, Denis Korably⁶⁷, Konstantin Kouzakov⁶⁹, Alexey Krasnoperov⁶⁷, Andre Kruth⁵¹, Nikolay Kutovskiy⁶⁷, Pasi Kuusiniemi⁴², Tobias Lachenmaier⁵⁴, Cecilia Landini⁵⁷, Sébastien Leblanc⁴⁴, Victor Lebrin⁴⁷, Frederic Lefevre⁴⁷, Ruiting Lei¹⁸, Rupert Leitner⁴¹, Jason Leung³⁸, Demin Li³⁷, Fei Li¹⁰, Fule Li¹³, Haitao Li²⁰, Huiling Li¹⁰, Jiaqi Li²⁰, Mengzhao Li¹⁰, Min Li¹¹, Nan Li¹⁰, Nan Li¹⁶, Qingjiang Li¹⁶, Ruhui Li¹⁰, Shanfeng Li¹⁸, Tao Li²⁰, Weidong Li^{10,14}, Weiguo Li¹⁰, Xiaomei Li⁹, Xiaonan Li¹⁰, Xinglong Li⁹, Yi Li¹⁸, Yufeng Li¹⁰, Zhaohan Li¹⁰, Zhibing Li²⁰, Ziyuan Li²⁰, Hao Liang⁹, Hao Liang²², Jiajun Liao²⁰, Daniel Liebau⁵¹, Ayut Limphirat⁷³, Sukit Limpijumnong⁷³, Guey-Lin Lin³⁸, Shengxin Lin¹⁸, Tao Lin¹⁰, Jiajie Ling²⁰, Ivano Lippi⁶⁰, Fang Liu¹¹, Haidong Liu³⁷, Hongbang Liu²⁸, Hongjuan Liu²³, Hongtao Liu²⁰, Hui Liu¹⁹, Jianglai Liu^{30,31}, Jinchang Liu¹⁰, Min Liu²³, Qian Liu¹⁴, Qin Liu²², Runxuan Liu^{50,48}, Shuangyu Liu¹⁰, Shubin Liu²², Shulin Liu¹⁰, Xiaowei Liu²⁰, Xiwen Liu²⁸, Yan Liu¹⁰, Yunzhe Liu¹⁰, Alexey Lokhov^{69,68}, Paolo Lombardi⁵⁷, Claudio Lombardo⁵⁵, Kai Loo⁵², Chuan Lu³², Haoqi Lu¹⁰, Jingbin Lu¹⁵, Junguang Lu¹⁰, Shuxiang Lu³⁷, Xiaoxu Lu¹⁰, Bayarto Lubsandorzhiev⁶⁸, Sultim Lubsandorzhiev⁶⁸, Livia Ludhova^{50,48}, Arslan Lukanov⁶⁸, Fengjiao Luo¹⁰, Guang Luo²⁰, Pengwei Luo²⁰, Shu Luo³⁶, Wuming Luo¹⁰, Vladimir Lyashuk⁶⁸, Bangzheng Ma²⁵, Qiumei Ma¹⁰, Si Ma¹⁰, Xiaoyan Ma¹⁰, Xubo Ma¹¹, Jihane Maalmi⁴³, Yury Malyshkin⁶⁷, Roberto Carlos Mandujano⁶⁷, Fabio Mantovani⁵⁶, Francesco Manzal⁶¹, Xin Mao⁷, Yajun Mao¹², Stefano M. Mari⁶⁴, Filippo Marini⁶¹, Sadia Marium⁶⁶, Cristina Martellini⁶⁴, Gisele Martin-Chassard⁴³, Agnese Martini⁶³, Matthias Mayer⁵³, Davit Mayilyan¹, Ints Mednieks⁶⁵, Yue Meng³⁰, Anselmo Meregaglia⁴⁴, Emanuela Meroni⁵⁷, David Meyhöfer⁴⁹, Mauro Mezzetto⁶⁰, Jonathan Miller⁶, Lino Miramonti⁵⁷, Paolo Montini⁶⁴, Michele Montuschi⁵⁶, Axel Müller⁵⁴, Massimiliano Nastasi⁵⁸, Dmitry V. Naumov⁶⁷, Elena Naumova⁶⁷, Diana Navas-Nicolás⁴³, Igor Nemchenok⁶⁷, Minh Thuan Nguyen Thi³⁸, Feipeng Ning¹⁰, Zhe Ning¹⁰, Hiroshi Nunokawa⁴, Lothar Oberauer⁵³, Juan Pedro Ochoa-Ricoux^{74,5}, Alexander Olshevskiy⁶⁷, Domizia Orestano⁶⁴, Fausto Ortica⁶², Rainer Othegraven⁵², Hsiao-Ru Pan⁴⁰, Alessandro Paoloni⁶³, Sergio Parmeggiani⁵⁷, Yatian Pei¹⁰, Nicomedè Pelliccia⁶², Anguo Peng²³, Haiping Peng²², Frédéric Perrot⁴⁴, Pierre-Alexandre Petitjean², Fabrizio Petrucci⁶⁴, Oliver Pilarczyk⁵², Luis Felipe Piñeres Rico⁴⁵, Artyom Popov⁶⁹, Pascal Poussot⁴⁵, Wathan Pratumwan⁷³, Ezio Previtali⁵⁸, Fazhi Qi¹⁰, Ming Qi²⁷, Sen Qian¹⁰, Xiaohui Qian¹⁰, Zhen Qian²⁰, Hao Qiao¹², Zhonghua Qin¹⁰, Shoukang Qiu²³, Muhammad Usman Rajput⁶⁶, Gioacchino Ranucci⁵⁷, Neill Raper²⁰, Alessandra Re⁵⁷, Henning Rebber⁴⁹, Abdel Rebiu⁴⁴, Bin Ren¹⁸, Jie Ren⁹, Barbara Ricci⁵⁶, Markus Robens⁵¹, Mathieu Roche⁴⁴, Narongkiat Rodphai⁷¹, Aldo Romani⁶², Bedřich Roskovec⁴¹, Christian Roth⁵¹, Xiangdong Ruan²⁸, Xichao Ruan⁹, Saroj Rujirawat⁷³, Arseniy Rybnikov⁶⁷, Andrey Sadovsky⁶⁷, Paolo Saggese⁵⁷, Simone Sanfilippo⁶⁴, Anut Sangka⁷², Nuanwan Sanguansak⁷³, Utane Sawangwit⁷², Julia Sawatzki⁵³, Fatma Sawy⁶¹, Michaela Schever^{50,48}, Cédric Schwab⁴⁵, Konstantin Schweizer⁵³, Alexandr Selyunin⁶⁷, Andrea Serafini⁵⁶, Giulio Settimo⁵⁰, Mariangela Settimio⁴⁷, Zhuang Shao³⁵, Vladislav Sharov⁶⁷, Arina Shaydurova⁶⁷, Jingyan Shi¹⁰, Yanan Shi¹⁰, Vitaly Shutov⁶⁷, Andrey Sidorenkov⁶⁸, Fedor Šimkovic⁷⁰, Chiara Sirignano⁶¹, Jaruchit Siripak⁷³, Monica Sisti⁵⁸, Maciej Słupecki⁴², Mikhail Smirnov²⁰, Oleg Smirnov⁶⁷, Thiago Sogo-Bezerra⁴⁷, Sergey Sokolov⁶⁷, Julianan Songwadhana⁷³, Boonrucksar Soonthornthum⁷², Albert Sotnikov⁶⁷, Ondřej Šrámek⁴¹, Warintorn Sreethawong⁷³, Achim Stahl⁴⁸, Luca Stanco⁶⁰, Konstantin Stankovich⁶⁹, Dušan Štefánik⁷⁰, Hans Steiger^{52,53}, Jochen Steinmann⁴⁸, Tobias Sterr⁵⁴, Matthias Raphael Stock⁵³, Virginia Strati⁵⁶, Alexander Studenikin⁶⁹, Shifeng Sun¹¹, Xilei Sun¹⁰, Yongjie Sun²², Yongzhao Sun¹⁰, Narumon Suwonjandee⁷¹, Michal Szelezniak⁴⁵, Jian Tang²⁰, Qiang Tang²⁰, Quan Tang²³, Xiao Tang¹⁰, Alexander Tietzsch⁵⁴, Igor Tkachev⁶⁸, Tomas Tmej⁴¹, Marco Danilo Claudio Torri⁴¹, Konstantin Treskov⁶⁷, Andrea Triossi⁴⁵, Giancarlo Troni⁵, Wladyslaw Trzaska⁴², Cristina

Tuve⁵⁵, Nikita Ushakov⁶⁸, Johannes van den Boom⁵¹, Stefan van Waasen⁵¹, Guillaume Vanroyen⁴⁷, Vadim Vedin⁶⁵, Giuseppe Verde⁵⁵, Maxim Vialkov⁶⁹, Benoit Viaud⁴⁷, Moritz Vollbrecht^{50,48}, Cristina Volpe⁴³, Vit Vorobel⁴¹, Dmitriy Voronin⁶⁸, Lucia Votano⁶³, Pablo Walker⁵, Caishen Wang¹⁸, Chung-Hsiang Wang³⁹, En Wang³⁷, Guoli Wang²¹, Jian Wang²², Jun Wang²⁰, Kunyu Wang¹⁰, Lu Wang¹⁰, Meifen Wang¹⁰, Meng Wang²³, Meng Wang²⁵, Ruiqiang Wang¹⁰, Siguang Wang¹², Wei Wang²⁷, Wei Wang²⁰, Wenshuai Wang¹⁰, Xi Wang¹⁶, Xiangyue Wang²⁰, Yangfu Wang¹⁰, Yaoguang Wang¹⁰, Yi Wang¹³, Yi Wang²⁴, Yifang Wang¹⁰, Yuanqing Wang¹³, Yuman Wang²⁷, Zhe Wang¹³, Zheng Wang¹⁰, Zhimin Wang¹⁰, Zongyi Wang¹³, Muhammad Waqas⁶⁶, Apimook Watcharangkool⁷², Lianghong Wei¹⁰, Wei Wei¹⁰, Wenlu Wei¹⁰, Yadong Wei¹⁸, Kaile Wen¹⁰, Liangjian Wen¹⁰, Christopher Wiebusch⁴⁸, Steven Chan-Fai Wong²⁰, Bjoern Wonsak⁴⁹, Diru Wu¹⁰, Qun Wu²⁵, Zhi Wu¹⁰, Michael Wurm⁵², Jacques Wurtz⁴⁵, Christian Wysotzki⁴⁸, Yufei Xi³², Dongmei Xia¹⁷, Xiaochuan Xie¹⁷, Yuguang Xie¹⁰, Zhangquan Xie¹⁰, Zhizhong Xing¹⁰, Benda Xu¹³, Cheng Xu²³, Donglian Xu^{31,30}, Fanrong Xu¹⁹, Hangkun Xu¹⁰, Jilei Xu¹⁰, Jing Xu⁸, Meihang Xu¹⁰, Yin Xu³³, Yu Xu^{50,48}, Baojun Yan¹⁰, Taylor Yan⁷³, Wenqi Yan¹⁰, Xiongbo Yan¹⁰, Yupeng Yan⁷³, Anbo Yang¹⁰, Changgen Yang¹⁰, Chengfeng Yang²⁸, Huan Yang¹⁰, Jie Yang³⁷, Lei Yang¹⁸, Xiaoyu Yang¹⁰, Yifan Yang¹⁰, Haifeng Yao¹⁰, Zafar Yasin⁶⁶, Jiaxuan Ye¹⁰, Mei Ye¹⁰, Ziping Ye³¹, Ugur Yegin⁵¹, Frédéric Yermia⁴⁷, Peihuai Yi¹⁰, Na Yin²⁵, Xiangwei Yin¹⁰, Zhengyun You²⁰, Boxiang Yu¹⁰, Chiye Yu¹⁸, Chunxu Yu³³, Hongzhao Yu²⁰, Miao Yu³⁴, Xianghui Yu³³, Zeyuan Yu¹⁰, Zezhong Yu¹⁰, Chengzhuo Yuan¹⁰, Ying Yuan¹², Zhenxiong Yuan¹³, Ziyi Yuan³⁴, Baobiao Yue²⁰, Noman Zafar⁶⁶, Andre Zambanini⁵¹, Vitalii Zavadskyi⁶⁷, Shan Zeng¹⁰, Tingxuan Zeng¹⁰, Yuda Zeng²⁰, Liang Zhan¹⁰, Aiqiang Zhang¹³, Feiyang Zhang³⁰, Guoqing Zhang¹⁰, Haiqiong Zhang¹⁰, Honghao Zhang²⁰, Jiawen Zhang¹⁰, Jie Zhang¹⁰, Jin Zhang²⁸, Jingbo Zhang²¹, Jinnan Zhang¹⁰, Peng Zhang¹⁰, Qingmin Zhang³⁵, Shiqi Zhang²⁰, Shu Zhang²⁰, Tao Zhang³⁰, Xiaomei Zhang¹⁰, Xuantong Zhang¹⁰, Xueyao Zhang²⁵, Yan Zhang¹⁰, Yinhong Zhang¹⁰, Yiyu Zhang¹⁰, Yongpeng Zhang¹⁰, Yuanyuan Zhang³⁰, Yumei Zhang²⁰, Zhenyu Zhang³⁴, Zhijian Zhang¹⁸, Fengyi Zhao²⁶, Jie Zhao¹⁰, Rong Zhao²⁰, Shujun Zhao³⁷, Tianchi Zhao¹⁰, Dongqin Zheng¹⁹, Hua Zheng¹⁸, Minshan Zheng⁹, Yangheng Zheng¹⁴, Weirong Zhong¹⁹, Jing Zhou⁹, Li Zhou¹⁰, Nan Zhou²², Shun Zhou¹⁰, Tong Zhou¹⁰, Xiang Zhou³⁴, Jiang Zhu²⁰, Kangfu Zhu³⁵, Kejun Zhu¹⁰, Zhihang Zhu¹⁰, Bo Zhuang¹⁰, Honglin Zhuang¹⁰, Liang Zong¹³ and Jiaheng Zou¹⁰

¹Yerevan Physics Institute, Yerevan, Armenia. ²Université Libre de Bruxelles, Brussels, Belgium. ³Universidade Estadual de Londrina, Londrina, Brazil. ⁴Pontificia Universidade Católica do Rio de Janeiro, Rio, Brazil. ⁵Pontificia Universidad Católica de Chile, Santiago, Chile. ⁶Universidad Técnica Federico Santa María, Valparaíso, Chile. ⁷Beijing Institute of Spacecraft Environment Engineering, Beijing, China. ⁸Beijing Normal University, Beijing, China. ⁹China Institute of Atomic Energy, Beijing, China. ¹⁰Institute of High Energy Physics, Beijing, China. ¹¹North China Electric Power University, Beijing, China. ¹²School of Physics, Peking University, Beijing, China. ¹³Tsinghua University, Beijing, China. ¹⁴University of Chinese Academy of Sciences, Beijing, China. ¹⁵Jilin University, Changchun, China. ¹⁶College of Electronic Science and Engineering, National University of Defense Technology, Changsha, China. ¹⁷Chongqing University, Chongqing, China. ¹⁸Dongguan University of Technology, Dongguan, China. ¹⁹Jinan University, Guangzhou, China. ²⁰Sun Yat-Sen University, Guangzhou, China. ²¹Harbin Institute of Technology, Harbin, China. ²²University of Science and Technology of China, Hefei, China. ²³The Radiochemistry and Nuclear Chemistry Group in University of South China, Hengyang, China. ²⁴Wuyi University, Jiangmen, China. ²⁵Shandong University, Jinan, China, and Key Laboratory of Particle Physics and Particle Irradiation of Ministry of Education, Shandong University, Qingdao, China. ²⁶Institute of Modern Physics, Chinese Academy of Sciences, Lanzhou, China. ²⁷Nanjing University, Nanjing, China. ²⁸Guangxi University, Nanning, China. ²⁹East China University of Science and Technology, Shanghai, China. ³⁰School of Physics and Astronomy, Shanghai Jiao Tong University, Shanghai, China. ³¹Tsung-Dao Lee Institute, Shanghai Jiao Tong University, Shanghai, China. ³²Institute of Hydrogeology and Environmental Geology, Chinese Academy of Geological Sciences, Shijiazhuang, China. ³³Nankai University, Tianjin, China. ³⁴Wuhan University, Wuhan, China. ³⁵Xi'an Jiaotong University, Xi'an, China. ³⁶Xiamen University, Xiamen, China. ³⁷School of Physics and Microelectronics, Zhengzhou University, Zhengzhou, China. ³⁸Institute of Physics, National Yang Ming Chiao Tung University, Hsinchu. ³⁹National United University, Miaoli. ⁴⁰Department of Physics, National Taiwan University, Taipei. ⁴¹Charles University, Faculty of Mathematics and Physics, Prague, Czech Republic. ⁴²University of Jyväskylä, Department of Physics, Jyväskylä, Finland. ⁴³IJCLab, Université Paris-Saclay, CNRS/IN2P3, 91405 Orsay, France. ⁴⁴Univ. Bordeaux, CNRS, CENBG, UMR 5797, F-33170 Gradignan, France. ⁴⁵IPHC, Université de Strasbourg, CNRS/IN2P3, F-67037 Strasbourg, France. ⁴⁶Centre de Physique des Particules de Marseille, Marseille, France. ⁴⁷SUBATECH, Université de Nantes, IMT Atlantique, CNRS-IN2P3, Nantes, France. ⁴⁸III. Physikalisches Institut B, RWTH Aachen University, Aachen, Germany. ⁴⁹Institute of Experimental Physics, University of Hamburg, Hamburg, Germany. ⁵⁰Forschungszentrum Jülich GmbH, Nuclear Physics Institute IKP-2, Jülich, Germany. ⁵¹Forschungszentrum Jülich GmbH, Central Institute of Engineering, Electronics and Analytics - Electronic Systems (ZEA-2), Jülich, Germany. ⁵²Institute of Physics, Johannes-Gutenberg Universität Mainz, Mainz, Germany. ⁵³Technische Universität München, München, Germany. ⁵⁴Eberhard Karls Universität Tübingen, Physikalisches Institut, Tübingen, Germany. ⁵⁵INFN Catania and Dipartimento di Fisica e Astronomia dell'Università di Catania, Catania, Italy. ⁵⁶Department of Physics and Earth Science, University of Ferrara and INFN Sezione di Ferrara, Ferrara, Italy. ⁵⁷INFN Sezione di Milano and Dipartimento di Fisica dell'Università di Milano, Milano, Italy. ⁵⁸INFN Milano Bicocca and University of Milano Bicocca, Milano, Italy. ⁵⁹INFN Milano Bicocca and Politecnico di Milano, Milano, Italy. ⁶⁰INFN Sezione di Padova, Padova, Italy. ⁶¹Dipartimento di Fisica e Astronomia dell'Università di Padova and INFN Sezione di Padova, Padova, Italy. ⁶²INFN Sezione di Perugia and Dipartimento di Chimica, Biologia e Biotecnologie dell'Università di Perugia, Perugia, Italy. ⁶³Laboratori Nazionali di Frascati dell'INFN, Roma, Italy. ⁶⁴University of Roma Tre and INFN Sezione Roma Tre, Roma, Italy. ⁶⁵Institute of Electronics and Computer Science, Riga, Latvia. ⁶⁶Pakistan Institute of Nuclear Science and Technology, Islamabad, Pakistan. ⁶⁷Joint Institute for Nuclear Research, Dubna, Russia. ⁶⁸Institute for Nuclear Research of the Russian Academy of Sciences, Moscow, Russia. ⁶⁹Lomonosov Moscow State University, Moscow, Russia. ⁷⁰Comenius University Bratislava, Faculty of Mathematics, Physics and Informatics, Bratislava, Slovakia. ⁷¹Department of Physics, Faculty of Science, Chulalongkorn University, Bangkok, Thailand. ⁷²National Astronomical Research Institute of Thailand, Chiang Mai, Thailand. ⁷³Suranaree University of Technology,

Nakhon Ratchasima, Thailand. ⁷⁴Department of Physics and Astronomy, University of California, Irvine, California, USA.

POS(ICRC2021)1229